Special Topic in Networks

Network Communicability: Properties, Extensions and Applications

Mostafa Mohsenvand
Mathematical Institute, University of Oxford

August 27, 2013

Abstract

This Special Topic essay is aimed to address various aspects, extensions and applications of the concept of Estrada's *Communicability* (EC) in networks. Here after a formal definition of EC in networks, mathematical properties of it are discussed. In particular, a new upper bound related to the edge cardinality of the network is provided for EC (in contrast with other bounds that only take the number of nodes into account). Then a new measure of communicability, Truncated Exponential Communicability (TEC) is introduced which has similar properties to EC and can bear more physical significance in modelling the information flow in networks. Then the concept of communicability distance is discussed and extended to TEC. Section applying binarizing filters on resulting distance matrices can recover the topology of the network and also be applicable in other related problems. For the rest of the essay, an application of network communicability and distance matrix binarization in neuroscience of stroke is presented and some new results based on recently developed functional imaging and optogenetical stimulation techniques are demonstrated.

Contents

Chapter 1

Communicability in Networks

1.1 Introduction

Over the past several years, the mathematical quantification of networks has become increasingly important in a number of fields. Network analysis is used in many situations: from determining network structure and communities, to describing the interactions between various elements of the network, to investigating the dynamics of phenomena taking place on the network (e.g. information flow, pandemics)[1, 2].

One of the fundamental questions in network analysis is to determine how nodes (which are not necessarily adjacent) in the network, interact with each other or in other words, how much an excitation in node v_i is felt in node v_j. The idea of communicability is devised by Estrada. et al [3] to be such a measure.

The intuition behind this concept is that in many real-world situations the communication between a pair of nodes in a network does not take place only through the optimal shortest-path routes connecting both nodes, but through all possible routes connecting both nodes, the number of which can be enormous in the complex networks. The information can also go back and forth before arriving at the end node of a given route. The network communicability quantifies such correlation effects in the communication between nodes in complex networks. The most important point that we will use to apply this concept to neuroscience applications is that the number of routes along which the correlation can grow is crucial in the analyses of the structures of complex networks.

From a physical point of view, calculation of communicability between two nodes is similar to performing a path integral between them where we compute a weighted sum of all possible paths in between. That is why communicability can be interpreted as the propagator (Green's function) of the network[4].

Now let us begin our discussion by providing a mathematical definition of communicability.

1.2 Mathematical Definition

Here we will define the concept of communicability using a combinatorial approach. Let us consider simple graphs $G = (V, E)$ with $|V| = n$ nodes and $|E| = m$ edges, undirected, unweighted, without self-loops and multiple edges between nodes.

Definition 1. *a **walk** of length k is a sequence of (not necessarily different) nodes, say indexed by $\{v_0, v_1, \cdots, v_{k-1}\}$ such that $\forall i = 1, \cdots, k, \{v_{i-1}, v_i\} \in E$.*

The adjacency matrix of a graph, denoted by $\mathbf{A}$, gives all the walks of length 1 between edges. To count the walks of higher length, one could compute the powers of $\mathbf{A}$ which are called moments.

Definition 2. *the **moment**, $\mu_k(p, q) \triangleq (\mathbf{A}^k)_{pq}$ gives the number of walks of length k from node p to q.*

Now a weighted sum of moments can be considered as a measure of communicability in the graph which in some sense, summarizes the connectivity information by generalizing the concept of shortest path. The main reasons for such a generalization is that in many networks which represent the information flow between nodes (e.g. neural , transportation and communication networks), the shortest path is not the only significant pathway between nodes and the actual interaction between nodes is carried out via multiple paths. The weighted sum of moments should penalize the paths with longer lengths in some way. Say if we give a general summation by:

$$\mathbf{G}_{pq} = \sum_{k=0}^{\infty} c_k \mu_k(p, q) = \sum_{k=0}^{\infty} c_k (\mathbf{A}^k)_{pq} \tag{1.1}$$

The coefficients c_k should be chosen in a way to: (i) penalize longer walks by giving less weight to them (or equivalently be proportional to a monotonically decaying function of k) , (ii) make sure the series 1.1 converges , and (iii) give a real positive value to the communicability as it is being considered as some sort of connectivity measure.

Polynomial candidates for c_k (e.g. $\frac{1}{k}, \frac{1}{k^2}, \cdots$)fail to satisfy the convergence requirement [3]. However, assuming an inverse factorial relationship fulfils all the needed properties. Hence we define:

Definition 3. *The **communicability** between nodes p and q is defined as:*

$$\mathbf{G}_{pq} = \sum_{k=0}^{\infty} \frac{(\mathbf{A}^k)_{pq}}{k!} = (e^{\mathbf{A}})_{pq} \tag{1.2}$$

The matrix exponential $(e^{\mathbf{A}})$ is defined as the matrix Taylor series of exponential function [3, 5]:

$$e^{\mathbf{A}} = \mathbf{I} + \mathbf{A} + \frac{\mathbf{A}^2}{2!} + \cdots + \frac{\mathbf{A}^k}{k!} + \cdots \tag{1.3}$$

The matrix $\mathbf{G} = e^{\mathbf{A}}$ is called the communicability matrix.

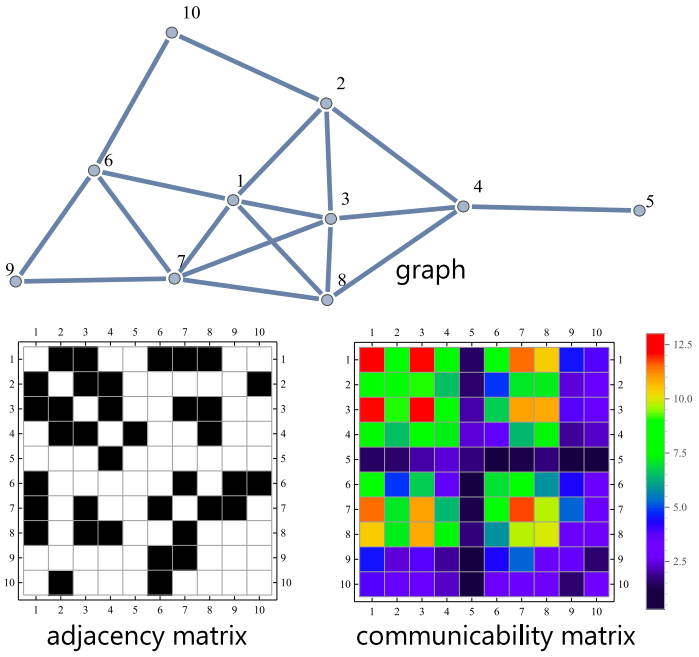

Figure 1.1: Graph → adjacency matrix → communicability matrix

Spectral decomposition or specifically Schur decomposition of $\mathbf{G}$ has a close relation with that of adjacency matrix (we will prove this in the next section):

$$\mathbf{G} = \mathbf{Q}e^{\mathbf{\Lambda}}\mathbf{Q}^T \qquad \text{where} \qquad \mathbf{A} = \mathbf{Q}\mathbf{\Lambda}\mathbf{Q}^T \tag{1.4}$$

or for a pair of nodes we can write:

$$\mathbf{G}_{pq} = \sum_{j=1}^{n} \phi_j(p)\phi_j(q)e^{\lambda_j}, \tag{1.5}$$

where $\phi_j(p)$ is the pth element of jth orthonormal eigenvector of $\mathbf{A}$ (or $(\mathbf{Q})_{pj}$) and λ_j is the jth eigenvalue of $\mathbf{A}$ [3].

1.3 The Bounds of Communicability

The matrix exponential is the most studied matrix function [5]. The interest in it stems from its crucial role in the solution of systems of differential equations which mostly appear in modern control theory. Depending on the application, the problem may be to compute $e^{\mathbf{A}}$ for a given $\mathbf{A}$, to compute $e^{\mathbf{A}t}$ for a fixed $\mathbf{A}$ and many t, or to apply $e^{\mathbf{A}}$ or $e^{\mathbf{A}t}$ to a vector [5].

To begin with, let us review some of the basic properties of matrix exponential. In the study of $e^{\mathbf{A}}$, two representations have seen to be useful. First the power series representation which we encountered in the previous section :

$$e^{\mathbf{A}} = \mathbf{I} + \mathbf{A} + \frac{\mathbf{A}^2}{2!} + \cdots + \frac{\mathbf{A}^k}{k!} + \cdots \tag{1.6}$$

Another representation is:

$$e^{\mathbf{A}} = \lim_{n\to\infty} (\mathbf{I} + \frac{1}{n}\mathbf{A})^n \tag{1.7}$$

This formula is the limit of the first order Taylor expansion of $\frac{1}{n}\mathbf{A}$ raised to the power $n \in \mathbb{N}$ [5].

As for the first property, we are going to show that matrix exponential is bounded for any bounded matrix. Therefore we need to show that $\|e^{\mathbf{A}}\| < \infty$ if $\|\mathbf{A}\| < \infty$ for any well-defined matrix norm. Here we will give the proof for Frobenius norm which is defined as: $\|\mathbf{A}\|_F = \sqrt{\sum_{i,j=1}^{n} A_{i,j}^2}$ where $\mathbf{A} \in \mathbb{R}^{n\times n}$.

Theorem 1. *[5] For $\mathbf{A} \in \mathbb{R}^{n\times n}$ and $\|\mathbf{A}\|_F < \infty$, the matrix exponential is bounded*

$$\|e^{\mathbf{A}}\|_F < \infty \tag{1.8}$$

Proof. Using the definition of Frobenius norm, for any matrix $\mathbf{B}$ with elements B_{ij} we have

$$|B_{ij}| \leq \|\mathbf{B}\|_F \qquad \text{and} \qquad \|\mathbf{B}^k\|_F \leq \|\mathbf{B}\|_F^k, \tag{1.9}$$

Now by taking $B = \dfrac{(\mathbf{A}^k)_{pq}}{k!}$ we can say:

$$(e^{\mathbf{A}})_{pq} = \sum_{k=0}^{\infty} \frac{(\mathbf{A}^k)_{pq}}{k!} \leq \sum_{k=0}^{\infty} \frac{\|\mathbf{A}^k\|_F}{k!} \leq \sum_{k=0}^{\infty} \frac{\|\mathbf{A}\|_F^k}{k!} = e^{\|\mathbf{A}\|_F} \tag{1.10}$$

which implies:

$$(e^{\mathbf{A}})_{pq} \leq e^{\|\mathbf{A}\|_F^k} \Longrightarrow \|e^{\mathbf{A}}\|_F \leq n e^{\|\mathbf{A}\|_F} \tag{1.11}$$

and as we have assumed $\|\mathbf{A}\|_F < \infty$, the series is convergent and the theorem is verified. □

This theorem gives rise to another theorem which bounds the root mean square of communicability (and therefore all other averages) of a simple graph as follows:

Theorem 2. [1] *The root mean square of the communicability in a network (G_{RMS}) with n nodes and m edges is bounded by:*

$$G_{RMS} \leq \frac{e^{\sqrt{2m}}}{n}$$

Proof. By definition:

$$G_{RMS} = \frac{1}{n^2}\|\mathbf{G}\|_F = \frac{1}{n^2}\|e^{\mathbf{A}}\|_F \tag{1.12}$$

now using Theorem 1 we can write:

$$G_{RMS} = \frac{1}{n^2}\|e^{\mathbf{A}}\|_F \leq \frac{e^{\|\mathbf{A}\|_F}}{n} \tag{1.13}$$

[1] This theorem is proved by the author of the essay and is original

However, for a simple graph we have $\|\mathbf{A}\|_F = \sqrt{2m(1)^2} = \sqrt{2m}$. Hence by considering the relationship between G_{RMS} and arithmetic mean ($\bar{G}$),geometric mean ($\hat{G}$) and harmonic mean (G_H) we get:

$$G_H \leq \hat{G} \leq \bar{G} \leq G_{RMS} \leq \frac{e^{\sqrt{2m}}}{n} \tag{1.14}$$

□

To find another bound and also to extend our discussion to the physical interpretation of communicability, let us prove the eigen-decomposition property of the exponential matrix.

Theorem 3. *The eigen-decomposition of matrix exponential $e^{\mathbf{A}}$ for a diagonalizable square matrix $\mathbf{A} \in \mathbb{R}^{n\times n}$ where $\mathbf{A} = \mathbf{P}\mathbf{\Lambda}\mathbf{P}^{-1}$ with eigenvalues $\mathbf{\Lambda} = \text{diag}(\lambda_1, \lambda_2, \cdots)$ is obtained by:*

$$e^{\mathbf{A}} = \mathbf{P}e^{\mathbf{\Lambda}}\mathbf{P}^{-1}$$

where $e^{\mathbf{\Lambda}} = \text{diag}(e^{\lambda_1}, e^{\lambda_2}, \cdots)$

Proof. Let us rewrite $\mathbf{A}^k$ using the given eigen-decomposition:

$$\mathbf{A}^k = (\mathbf{P}\mathbf{\Lambda}\mathbf{P}^{-1})^k = \overbrace{\mathbf{P}\mathbf{\Lambda}\underbrace{\mathbf{P}^{-1}\mathbf{P}}_{\mathbf{I}}\mathbf{\Lambda}\underbrace{\mathbf{P}^{-1}\mathbf{P}}_{\mathbf{I}}\cdots\underbrace{\mathbf{P}^{-1}\mathbf{P}}_{\mathbf{I}}\mathbf{\Lambda}\underbrace{\mathbf{P}^{-1}\mathbf{P}}_{\mathbf{I}}\mathbf{\Lambda}\mathbf{P}^{-1}}^{\text{k times}} \tag{1.15}$$

Which gives:

$$\mathbf{A}^k = \mathbf{P}\mathbf{\Lambda}^k\mathbf{P}^{-1} \tag{1.16}$$

Now by putting back everything into the series we will have:

$$e^{\mathbf{\Lambda}} = \sum_{k=0}^{\infty}\frac{\mathbf{A}^k}{k!} = \sum_{k=0}^{\infty}\frac{\mathbf{P}\mathbf{\Lambda}^k\mathbf{P}^{-1}}{k!} = \mathbf{P}e^{\mathbf{\Lambda}}\mathbf{P}^{-1} \tag{1.17}$$

and also we know that for a diagonal matrix $\mathbf{\Lambda} = \text{diag}(\lambda_1, \lambda_2, \cdots)$

$$\mathbf{\Lambda}^k = \text{diag}(\lambda_1^k, \lambda_2^k, \cdots) \tag{1.18}$$

hence we get:

$$e^{\mathbf{\Lambda}} = \text{diag}(e^{\lambda_1}, e^{\lambda_2}, \cdots) \tag{1.19}$$

□

One useful remark on the Theorem 3 can be made by considering the fact that adjacency matrix of simple graphs is symmetric which implies the existence of Schur decomposition where instead of $\mathbf{P}$ and $\mathbf{P}^{-1}$ we can replace orthogonal matrices $\mathbf{Q}$ and $\mathbf{Q}^T$: $\mathbf{A} = \mathbf{Q}\mathbf{\Lambda}\mathbf{Q}^T \Rightarrow e^{\mathbf{A}} = \mathbf{Q}e^{\mathbf{\Lambda}}\mathbf{Q}^T$. In [3] Estrada et al. use the Schur decomposition of the adjacency matrix of complete graphs to establish other bounds on the communicability. However, they fail to calculate the communicability matrix of a complete graph accurately. Here we will use another property of matrix exponential to achieve our goal.

Theorem 4. *If two matrices* $\mathbf{A} \in \mathbb{R}^{n\times n}$ *and* $\mathbf{B} \in \mathbb{R}^{n\times n}$ *commute (i.e.* $[\mathbf{A}, \mathbf{B}] = \mathbf{AB} - \mathbf{BA} = \mathbf{0}$*) then we have:*

$$e^{\mathbf{A}+\mathbf{B}} = e^{\mathbf{A}} e^{\mathbf{B}}$$

Proof. The commutation of matrices allows us to treat them as scaler numbers. Therefore, by writing binomial expansion, the proof will be straightforward. For detailed proof look at [5]. □

Now let's use this theorem to calculate the communicability matrix of a complete graph. First we need to establish a lemma:

Lemma 1. *Matrix exponential of an all-one square matrix (*$\mathbf{1}_n \in \mathbb{R}^{n\times n}$: $(\mathbf{1}_n)_{ij} = 1\ \forall i, j = 1 \cdots n$*) is obtained by:*

$$e^{\mathbf{1}_n} = \mathbf{I} + \frac{e^n - 1}{n}\mathbf{1}_n$$

Proof. noting that $\mathbf{1}_n^k = n^{k-1}\mathbf{1}_n$ we have:

$$e^{\mathbf{1}_n} = \sum_{k=0}^{\infty} \frac{\mathbf{1}_n^k}{k!} = \mathbf{I} + \sum_{k=1}^{\infty} \frac{n^{k-1}\mathbf{1}_n}{k!} = \mathbf{I} + \frac{e^n - 1}{n}\mathbf{1}_n \tag{1.20}$$

□

As the adjacency matrix of a complete graph with n nodes can be constructed as $\mathbf{K}_n = \mathbf{1}_n - \mathbf{I}$ (i.e. all-one except diagonal elements equal to 0) we can calculate the communicability matrix it using Theorem 4 and Lemma 1 as follows:

Theorem 5. *The communicability matrix of a complete graph of size* n *with adjacency matrix* $\mathbf{K}_n = \mathbf{1}_n - \mathbf{I}$ *is:*

$$e^{\mathbf{K}_n} = \frac{1}{e}\left(\mathbf{I} + \frac{e^n - 1}{n}\mathbf{1}_n\right)$$

Proof. Using Theorem 4 and considering the fact that $-\mathbf{I}$ commutes with all equidimensional matrices and $e^{-\mathbf{I}} = \frac{1}{e}(\mathbf{I})$, we have:

$$e^{\mathbf{K}_n} = e^{\mathbf{1}_n - \mathbf{I}} = e^{-\mathbf{I}} e^{\mathbf{1}_n} = \frac{1}{e}\left(\mathbf{I} + \frac{e^n - 1}{n}\mathbf{1}_n\right) \tag{1.21}$$

or element-wise we have:

$$(e^{\mathbf{K}_n})_{ij} = \begin{cases} \frac{e^n - 1}{ne} & i \neq j \\ \frac{e^n - 1 + n}{ne} & i = j \end{cases} \tag{1.22}$$

□

Intuitively, complete graphs are the most connected ones. Hence cross-communicability and self-communicability of a complete graph with n nodes is an upper bound for communicability of all the graphs of n nodes regardless of number of edges. Moreover, Theorem 1 shows that the communicability increases with the number of edges which confirms the intuitive deduction as complete graphs have the maximum number of edges.

1.4 Communicability for Directed and Weighted Graphs

The concept of communicability can be easily extended to directed and weighted networks by taking the matrix exponential of their adjacency matrix. In general case of weighted networks, a normalization of adjacency matrix is recommended. Based on the work of Crofts and Higham [6], we have:

$$\tilde{\mathbf{G}} = e^{\mathbf{W}^{-1/2}\mathbf{A}\mathbf{W}^{-1/2}} \tag{1.23}$$

Where $\mathbf{A}$ is the weighted adjacency matrix and $\mathbf{W}$ is the diagonal matrix of degrees. This definition of weighted communicability has been shown to be applicable in the applications of neuroscience and connectomics. In the next section, we will introduce a new form of communicability function which may have more physical implications.

1.5 Truncated Exponential Communicability for Weighted Graphs

Lets assume that our network is kind of communication network in which nodes can communicate through signals which get linearly attenuated before being received. That is, every link in the network has an effect on the signal being transmitted modelled by a Beer-Lambert law :

$$I_j = I_i e^{-\alpha_{ij} w_{ij}} \tag{1.24}$$

where I_i and I_j are the intensity of the signal at the transmitting and receiving nodes respectively. $w_i j$ is a relevant form of distance between nodes which can be replaced by a function of the weights of the edges and $\alpha_{ij} > 0$ is called the attenuation coefficient of the link from i to j and models the physical properties of the link and it can be asymmetric in case of media with polarity(e.g. neurons). Evidently, as the distance between nodes (w_{ij}) gets larger, received signal gets exponentially weaker. Keeping this model in mind, let us define another measure of communicability:

Definition 4. *For a weighted graph G with adjacency matrix $\mathbf{A}$ the truncated exponential communicability (TEC) of order $N \in \mathbb{N}$ is defined as*

$$\boldsymbol{\mathcal{C}}_N = \sum_{k=0}^{N} (\mathbf{E} - \mathbf{B})^k \tag{1.25}$$

where elements of $\mathbf{E}$ are negative exponentials of $\mathbf{A}$:

$$(\mathbf{E})_{ij} = \exp[-(\mathbf{A}^T)_{ij}] \tag{1.26}$$

and $\mathbf{B}$ is the logical not *of transpose of adjacency matrix ($\mathbf{B} = \neg\mathbf{A}^{\mathbf{T}}$) which can be written as:*

$$(\mathbf{B})_{ij} = \begin{cases} 0 & (\mathbf{A})_{ji} \neq 0 \\ 1 & (\mathbf{A})_{ji} = 0 \end{cases} \tag{1.27}$$

A wise choice of N is the diameter of the graph $d(G)$ to make sure all nodes effect each other. In this case, we will drop N from the notation:

$$\mathcal{C} = \sum_{k=0}^{d(G)} (\mathbf{E} - \mathbf{B})^k \tag{1.28}$$

To illustrate an example of application of $\mathcal{C}^N$, consider the graph in Figure 1.2 with adjacency matrix given by 1.29.

$$\mathbf{A} = \begin{pmatrix} 0 & w_{12} & w_{13} \\ w_{21} & 0 & w_{23} \\ w_{31} & w_{32} & 0 \end{pmatrix} \tag{1.29}$$

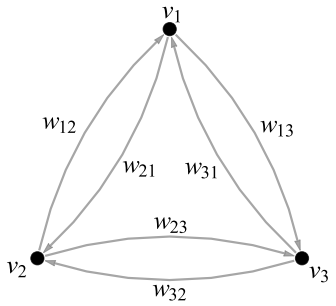

Figure 1.2: Weighted K_3

Now let us suppose there are three sources of signal with intensities $\mathbf{S} = (I_1, I_2, I_3)^T$ located at corresponding nodes of the graph and suppose the intensity of signal at each node obeys a Beer-Lambert law with superposition and $\alpha_{ij} = 1$.
Another crucial assumption that is to be made is considering that the signal will completely dissipate after a certain number of send/receives (here N), which means, the network will not be able to detect the signal due to multiple attenuations. Then the intensity of the signal at nodes can be calculated as:

$$\hat{\mathbf{S}}^N = \mathcal{C}^N \mathbf{S} \tag{1.30}$$

for example for the graph above, with $N = 0, 1, 2, 3$ (maximum number of times that the signal can be sensed and sent), the intensity at node v_1 is:

$$\begin{array}{ll}
N = 0, & \hat{I}_1^0 = I_1 \\
\hline
N = 1, & \hat{I}_1^1 = I_1 + I_2 e^{-w_{21}} + I_3 e^{-w_{31}} \\
\hline
N = 2, & \hat{I}_1^2 = I_1 + I_2 e^{-w_{21}} + I_3 e^{-w_{31}} \\
 & \quad + I_1(e^{-(w_{12}+w_{21})} + e^{-(w_{13}+w_{31})}) \\
 & \quad + I_2(e^{-(w_{23}+w_{31})}) + I_3(e^{-(w_{21}+w_{32})}) \\
\hline
N = 3, & \hat{I}_1^3 = I_1 + I_2 e^{-w_{21}} + I_3 e^{-w_{31}} \\
 & \quad + I_1(e^{-(w_{12}+w_{21})} + e^{-(w_{13}+w_{31})}) \\
 & \quad + I_2(e^{-(w_{23}+w_{31})}) + I_3(e^{-(w_{21}+w_{32})}) \\
 & \quad + I_1(e^{-(w_{12}+w_{23}+w_{31})} + e^{-(w_{13}+w_{21}+w_{32})}) \\
 & \quad + I_2(e^{-(w_{12}+2w_{21})} + e^{-(w_{23}+w_{32}+w_{21})} + e^{-(w_{13}+w_{21}+w_{31})}) \\
 & \quad + I_3(e^{-(w_{13}+2w_{31})} + e^{-(w_{23}+w_{32}+w_{31})} + e^{-(w_{12}+w_{21}+w_{31})})
\end{array}$$

Which is exactly what we would like to get as the super position of all send/receives with appropriate attenuations. Figure 1.3 shows all the paths that signal gets transmitted to v_1 for $N = 2$.

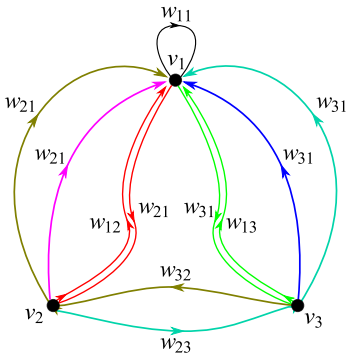

$$\hat{I}_1 = I_1 + I_2 e^{-w_{21}} + I_3 e^{-w_{31}} + I_1 e^{-(w_{12}+w_{21})} + I_1 e^{-(w_{13}+w_{31})} + I_2 e^{-(w_{23}+w_{31})} + I_3 e^{-(w_{21}+w_{32})}$$

Figure 1.3: Superposed signal intensity at v_1 : $(\hat{\mathbf{S}}_2)_1 = (\boldsymbol{\mathcal{C}}^2\mathbf{S})_1$

Evidently, TEC is a physically meaningful concept and its application on a vector has a clear meaning and application. But how is it compared to the usual communicability ($\mathbf{G}$) ? Figure 1.4.a shows the element-wise 1-norm difference of normalized communicability and TEC($N = 10$) for the graph shown in Figure 1.1. As you see the element-wise difference is extremely small. Figure 1.4.b compares two communicability measures in matrix 2-norm and frobinus norm.

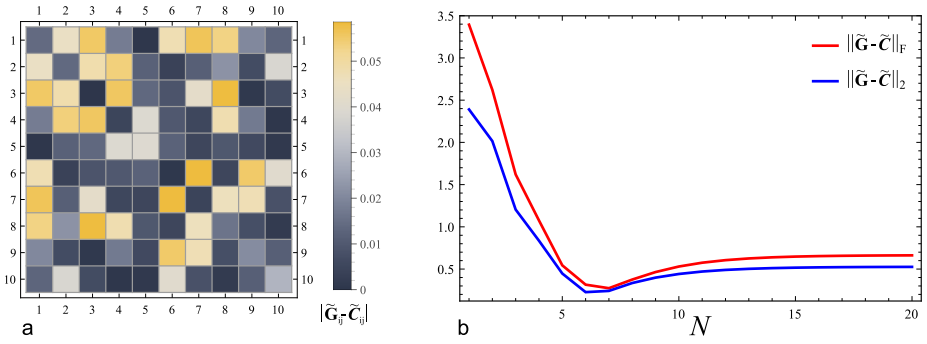

Figure 1.4: TEC($\boldsymbol{\mathcal{C}}$) and Estrada Communicability($\mathbf{G}$) are very close

1.6 Communicability Distance

In this section we are interested in analysing how much of an activity/excitation is received by the pairs of nodes and how much of it is transmitted from one to the other. The physical intuition behind the definition of communicability distance is that if there is a thermal disturbance to the whole network, how large is the difference between the absorbed and transmitted excitation between two nodes?

Communicability distance is defined by Estrada et al. in [7] and is given by the following definition.

Definition 5. *For a graph with communicability matrix* $\mathbf{G}$*, the* ***communicability distance*** *between two nodes* p *and* q *is defined by:*

$$\xi_{pq}^2 = \mathbf{G}_{pp} + \mathbf{G}_{qq} - 2\mathbf{G}_{pq} \tag{1.31}$$

Considering the eigen-decomposition of $\mathbf{G}$ as in:

$$\mathbf{G}_{pq} = \sum_{j=1}^{n} \phi_j(p)\phi_j(q)e^{\lambda_j},$$

Here we show that ξ_{pq} acts like the Euclidean distance between two vectors $\boldsymbol{\phi}_p e^{\boldsymbol{\Lambda}/2}$ and $\boldsymbol{\phi}_q e^{\boldsymbol{\Lambda}/2}$.

Theorem 6. *[7] Given* $\mathbf{x}_p = \boldsymbol{\phi}_p e^{\boldsymbol{\Lambda}/2}$ *and* $\mathbf{x}_q = \boldsymbol{\phi}_q e^{\boldsymbol{\Lambda}/2}$*:*

$$\xi_{pq} = \sqrt{\|\mathbf{x}_p - \mathbf{x}_q\|}$$

Proof. let's rewrite ξ_{pq}^2 as in

$$\xi_{pq}^2 = (\boldsymbol{\phi}_p - \boldsymbol{\phi}_q)^T e^{\boldsymbol{\Lambda}}(\boldsymbol{\phi}_p - \boldsymbol{\phi}_q) \tag{1.32}$$

and regroup it as

$$\begin{aligned} \xi_{pq}^2 &= (e^{\boldsymbol{\Lambda}/2}(\boldsymbol{\phi}_p - \boldsymbol{\phi}_q))^T e^{\boldsymbol{\Lambda}/2}(\boldsymbol{\phi}_p - \boldsymbol{\phi}_q) && (1.33)\\ &= (e^{\boldsymbol{\Lambda}/2}\boldsymbol{\phi}_p - e^{\boldsymbol{\Lambda}/2}\boldsymbol{\phi}_q)^T (e^{\boldsymbol{\Lambda}/2}\boldsymbol{\phi}_p - e^{\boldsymbol{\Lambda}/2}\boldsymbol{\phi}_q) && (1.34) \end{aligned}$$

now using the definition of $\mathbf{x}_p$ and $\mathbf{x}_q$ we have

$$\begin{aligned} \xi_{pq} &= (\mathbf{x}_p - \mathbf{x}_q)^T (\mathbf{x}_p - \mathbf{x}_q) && (1.35)\\ &= \sqrt{\|\mathbf{x}_p - \mathbf{x}_q\|} && (1.36) \end{aligned}$$

Therefore ξ_{pq} behaves like euclidean distance and has all its properties. □

Communicability distance can also be defined for TEC in the same way. We define:

Definition 6. *For a graph with TEC matrix* $\boldsymbol{\mathcal{C}}^N$*, the* ***TEC distance*** *between two nodes* p *and* q *is defined by:*

$$(\mathcal{D}_{pq}^N)^2 = \boldsymbol{\mathcal{C}}_{pp}^N + \boldsymbol{\mathcal{C}}_{qq}^N - \boldsymbol{\mathcal{C}}_{pq}^N \tag{1.37}$$

Chapter 2

Distance Matrix Binarization(DMB)

In this section we will introduce the idea of distance matrix binarization (DMB) by an example. Next we will provide a mathematical definition of it and show its non-trivial application for dealing with communicability distance matrices.

2.1 Second Neighbour connectivity: an example for DMB

Let us begin with a straightforward example. Take a 5×5 grid graph as shown in Figure 2.1. This graph is obviously connected (i.e there exists a path between

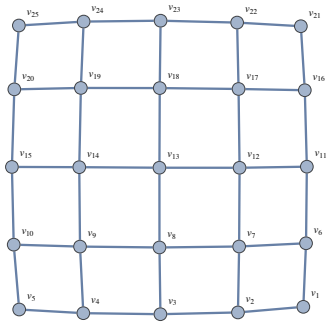

Figure 2.1: Grid graph (5×5)

each pair of nodes in the graph). Now imagine we can only move in steps of length 2 ,that is, if we are at node v_i and want to crawl the graph, we can only jump to one of our second neighbours. But will be able to pass all the nodes starting from any initial node? In other words, is the graph still connected with step-size 2? Let's try it by moving from v_1 to v_2. It is impossible,therefore, the graph is not connected with step-size 2. Here we propose an obvious way to find the l-step model of the graph by binarization of the distance matrix of the

graph. Here we give the adjacency matrix of the resulting graph by

$$\left(\mathbf{A}^{G}_{\mathcal{B}_l}\right)_{ij} = \mathcal{B}_l(d_{ij}) \qquad \text{where } d_{ij} = [\mathbf{D}]_{ij}. \tag{2.1}$$

Here $\mathcal{B}_l$ is a *binarization method* which is defined as a function of distance matrix and for this simple case is:

$$\mathcal{B}_l(d) = \begin{cases} 1 & d = l \\ 0 & otherwise \end{cases} \tag{2.2}$$

Equation 2.1 takes the distance matrix $\mathbf{D}$ of the graph G and discards all the elements which are not equal to l and mapped the rest to 1. Figure 2.2 shows the distance matrix of our grid graph and the binarized output of Equation 2.1.

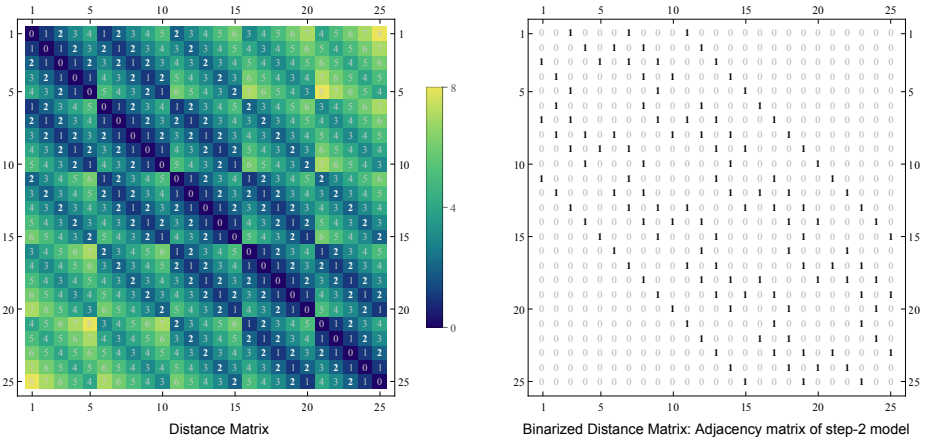

Figure 2.2: The effect of DMB algorithm, $\mathbf{D} \rightarrow \mathbf{A}_2$

Now by taking the resulted matrix as the adjacency matrix we will have a new graph. Visualization of $\mathbf{A}_2$ gives a disconnected graph as we speculated before. Figure 2.3 shows the resulting graph. As we see, the nodes v_1 and v_2 are in disconnected sub-graphs.

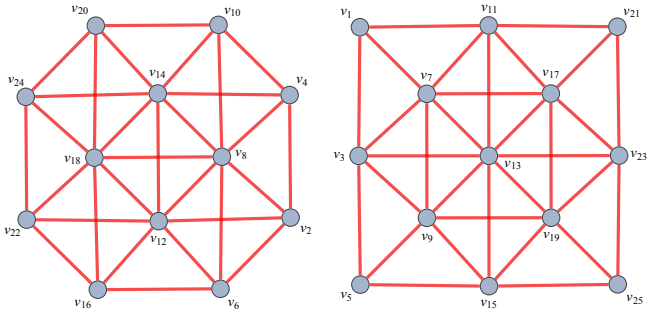

Figure 2.3: step-2 model of the 5×5 grid graph. Red edges show the 2-step connectivity between nodes

Obviously for $l = 1$ the method gives the adjacency graph of the matrix and the resulting graph would be identical.

2.2 Communicability Distance Matrix Binarization (CDMB)

Here we will give a general definition of Distance Matrix Binarization.

Definition 7. *a **binarization method** $\mathcal{B}(d_{ij})$ is a function that maps elements of distance matrix $d_{ij} = (\mathbf{D})_{ij}$ to the set $\{0, 1\}$. A **distance matrix binarization model** (DMBM) of the graph G using the binarization method $\mathcal{B}$ is the graph $F^G_{\mathcal{B}}$ which is defined by its adjacency matrix as:*

$$\left(\mathbf{A}^G_{\mathcal{B}}\right)_{ij} = \mathcal{B}(d_{ij}) \tag{2.3}$$

Here F stands for filter *as the operation is similar to the filtering of images.*

The non-trivial application of DMB becomes evident when dealing with other distance metrics on the network. In this section, we will show the result of DMB on two different distance matrices Estrada communicability distance matrix $\boldsymbol{\xi}$ and TEC distance matrix $\boldsymbol{\mathcal{D}}^N$.

One possible application is to recover the topology of the network based on distance or correlation data coming from the interaction of nodes. As an example, let us introduce a thresholding binarization method which maps all the distances in a certain interval to 1 and the rest to zero or mathematically:

$$\mathcal{B}_{\theta_L,\theta_H}(d) = \begin{cases} 1 & \theta_L \leq d \leq \theta_H \\ 0 & otherwise \end{cases} \tag{2.4}$$

Now let us take the graph in 2.4.a as an example. Figure 2.4.b, 2.4.c ,2.4.d and 2.4.e show its adjacency matrix, normalized distance matrix, normalized Estrada distance matrix and normalized TEC distance matrices respectively.

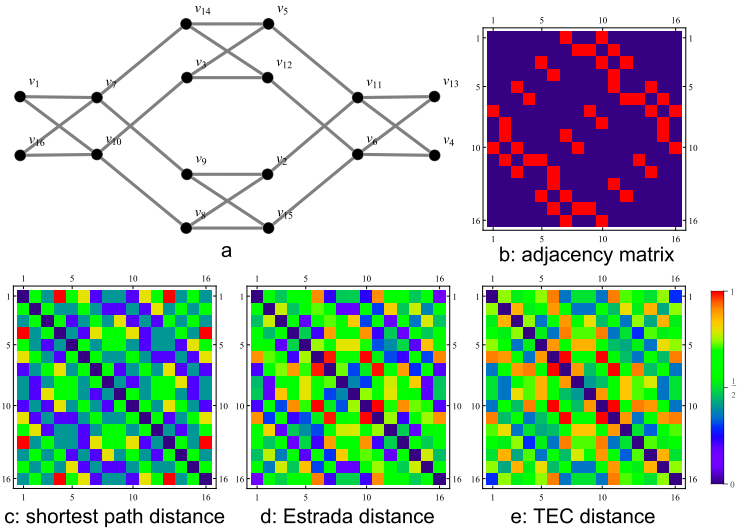

Figure 2.4: Knight Tour Graph (4×4), and three distance matrices

Figure 2.5 and Figure 2.6 demonstrates DMB of this graph using $\boldsymbol{\xi}$ and $\boldsymbol{\mathcal{D}}$ ($N = d(G)$) for different thresholding intervals:

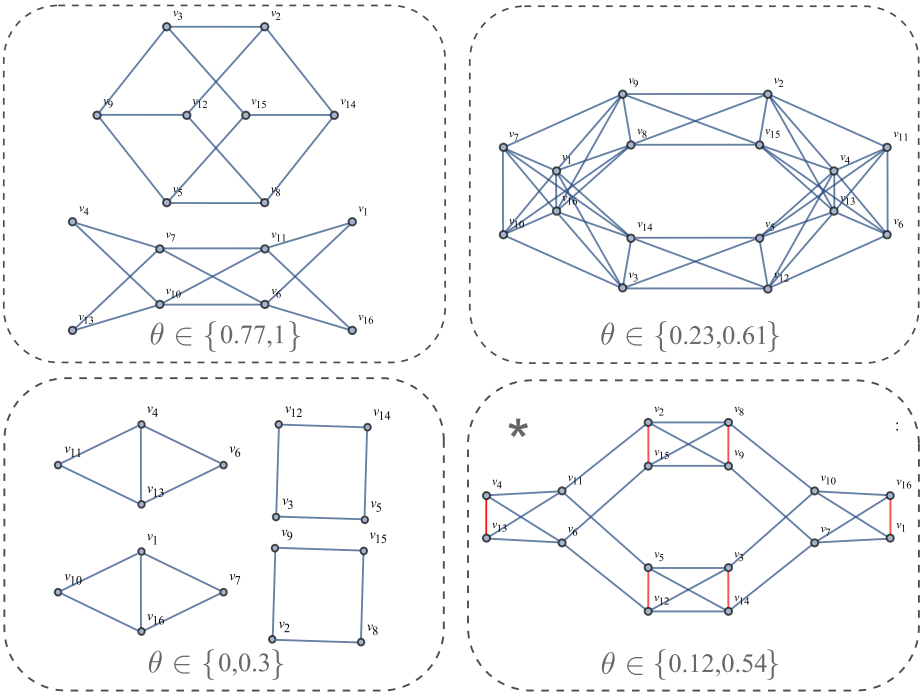

Figure 2.5: DMB using Estrada Distance

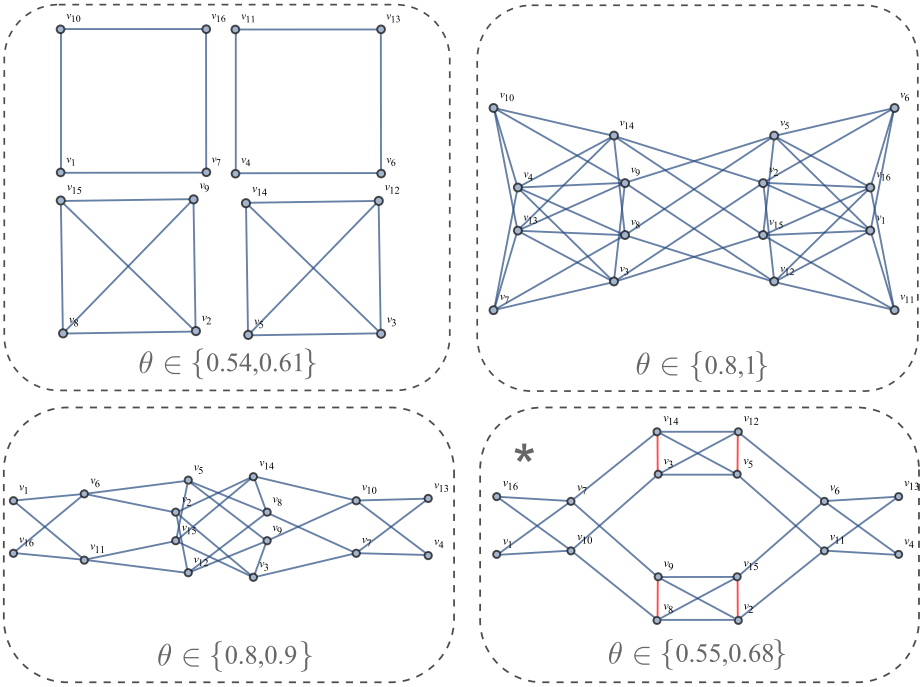

Figure 2.6: DMB using TEC Distance

Considering the details of Figure 2.5.* and 2.6.* , we observe that binarization of communicability distance matrix can approximately recover the topology of the original graph. Indeed for simple classes of networks like paths, rings and grids, CDMB recovers the network exactly. Figure 2.7 shows the exact recovery of a Grid graph using CDMB by Estrada distance.

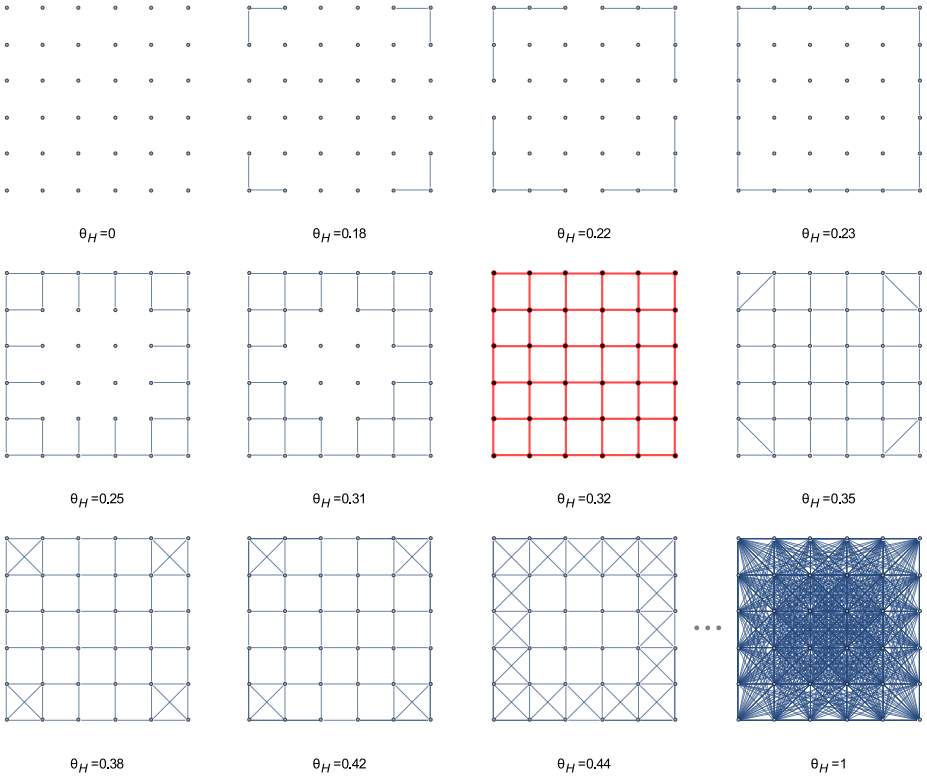

Figure 2.7: Recovery of a grid graph by binarization of its Estrada distance matrix. Here $\theta_L = 0$

This recovery property will be very useful when we only have information about either communicability (correlation) or distance of nodes and do not know the topology of the network. In the next section, we are going to make use of this method to detect the connectivity of brain neural networks when we only know the correlation of neurons.

Chapter 3

Applications in Neuroscience

Sebastian Seung, an MIT Physicist and Neuroscientist has popularized the motto *I am my connectome*, that basically means: every complex aspect of human behaviour is coded in the connectivity pattern of neurons in the brain[8]. Detecting the connectivity of neurons and monitoring its changes under pathological conditions or developmental processes is an extremely challenging task. Mathematical tools and techniques developed in the area of network science can be applied to these problems[2, 1, 9]. There are myriad papers on applications of network science in the study of nervous systems which shows that these approaches are exceptionally powerful in characterizing structural and functional brain networks. To begin with explaining our desired application, a general description of the structure of the brain does not hurt.

The brain is divided up into cortical areas which in many macroscopic and mesoscopic models are taken as the nodes of the network where edges are modelled as white matter fibres (Section 3.1) or by functional correlation between areas (Section 3.2). In some microscopic models, every single neuron is considered as a node and links represent synaptic connections in between.

In the next section we will review the application of Communicability in identification of changes in the connectivity of the human brain after stroke where data is collected using DTI technique. Next we will discuss a much more reliable data acquisition method (VSD + Optogenetics)and will demonstrate the results of application of communicability analysis on that data.

3.1 Previous Results on Identification of Stroke Lesions using Communicability

Anatomical and functional alterations in brain structure occur in distant regions after stroke. Such changes could spread across widely distributed brain networks. In the research done by Crofts et al. [9, 6] they used diffusion MRI tractography to assess connectivity between brain regions in chronic stroke patients and age-matched controls.
They applied Estrada's communicability analysis to measure the permeability

with which information can travel across the network. Their work showed that communicability analysis can be successfully used to cluster individuals into patient and control groups, not only in the lesioned hemisphere but also in the contralesional hemisphere, despite the absence of gross structural pathology in the latter.

The strategy was to select a group of whom, lesions were localised to the a certain brain area (left basal ganglia/internal capsule). The study showed that reduced communicability in patients in regions surrounding the lesions in the affected hemisphere. In addition, communicability was reduced in homologous locations in the contralesional hemisphere for a subset of these regions.

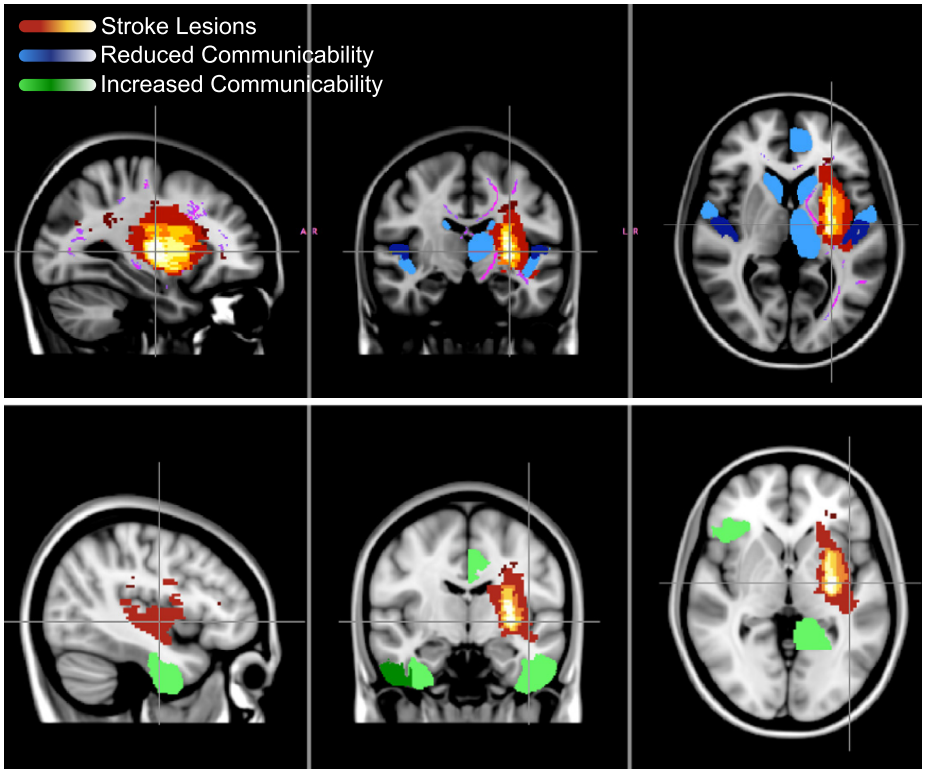

Figure 3.1: Communicability changes after stroke. Taken from [9] with courtesy

They interpreted this as evidence for secondary degeneration of fibre pathways which occurs in remote regions interconnected, directly or indirectly, with the area of primary damage. They also identified regions with increased communicability in patients that could represent adaptive, plastic changes post-stroke.

In their work, connectivity information, which is provided by the probabilistic tractography step, takes the from of real-valued, positive weights. Where a larger weight a_{ij} indicates a greater *strength* of connection between nodes i and j (note that strength simply refers to the number of tractography streamlines that connect two nodes, and does not relate in a straightforward way to anatomical strength of connection). However, for calculating communicability, rather than simply making a zero/one contribution depending upon whether the walk $v_i \to r_1 \to r_2 \to \cdots r_{k1} \to v_j$ is possible, the term $a_{i,r_1} a_{r_1 r_2} a_{r_{k2} r_{k1}} a_{r_{k1} j}$

contributes the product of the weights along all the edges in the walk. To avoid difficulties which may arise if the weights are poorly calibrated, instead of usual definition of communicability, they have used the normalized communicability formula as we discussed in Section 1.5.(look at Equation 1.23). If the unnormalized is used, nodes with unusually large weights typically dominate the results.

The results showed evidence for reduced communicability in patients in the contralesional hemisphere (see Figure 3.1 upper row). These areas in the contralesional hemisphere are remote from the site of primary damage, but are anatomically connected, directly or indirectly, with their homologues in the lesioned hemisphere

This pattern of reduced communicability shows some similarities to previously reported patterns of secondary degeneration detected using other imaging modalities or measures. In addition to regions of reduced communicability, they also found some areas of greater communicability in patients compared to controls (see Figure 3.1 bottom row).

One possible interpretation of these changes is that increased communicability reflects adaptive changes in white matter structure that have occurred secondary to the stroke. An alternative hypothesis is that the changes predated the lesion and represent a marker of stroke risk.

3.2 Optogenetics+VSD

3.2.1 Optogenetics

To better understand the connectivity of the brain, it is important to map both structural and functional connections between neurons and cortical regions [12]. In recent years, a set of optogenetic and imaging tools have been developed that permit selective manipulation and investigation of neural systems. These tools have enabled the mapping of functional connections between stimulated cortical targets and other brain regions. Advantages of the approach include the ability to *arbitrarily stimulate brain regions* that express opsins, allowing for brain mapping independent of behavior or sensory processing [12]. The ability of opsins to be rapidly and locally activated allows for investigation of connectivity with spatial resolution on the order of single neurons and temporal resolution on the order of milliseconds.

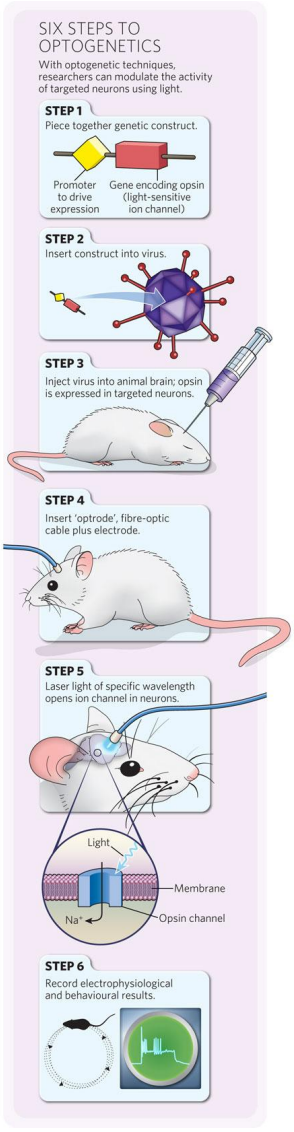

Figure 3.2: Optogenetics, from [12]

Optogenetic methods for functional mapping have been applied in experiments ranging from in vitro investigation of microcircuits, to in vivo probing of inter-regional cortical connections, to examination of global connections

within the whole brain (see Figure 3.2). Here we focus on recently developed functional mapping methods that use optogenetic single-point stimulation in the rodent brain and voltage sensitive dyes (VSDs) to assess activity. In particular we highlight results using red-shifted organic VSDs that permit high temporal resolution imaging in a manner spectrally separated from Channelrhodopsin-2 (ChR2) activation. VSD maps stimulated by ChR2 were dependent on intracortical synaptic activity and were able to reflect circuits used for sensory processing.

3.2.2 Voltage Sensitive Dye Imaging

Voltage sensitive dye (VSD) imaging is one method for investigating large-scale cortical ensemble activity and long-range connections in vivo [10]. VSDs are membrane-bound, organic, small molecules that are used to monitor membrane potential changes through various biophysical mechanisms, with the simplest mechanism being redistributionthe VSD incorporates into the cell membrane and changes in membrane potential cause the dye molecule to move into or out of the membrane, leading to relatively linear changes in the fluorescence or absorbance of the dye. VSD imaging has potentially diffraction-limited spatial resolution and high temporal resolution. Furthermore, VSD imaging does not filter for activity based on spiking, but reports membrane potential changes, so it reflects supra- and subthreshold neuronal activity[10].

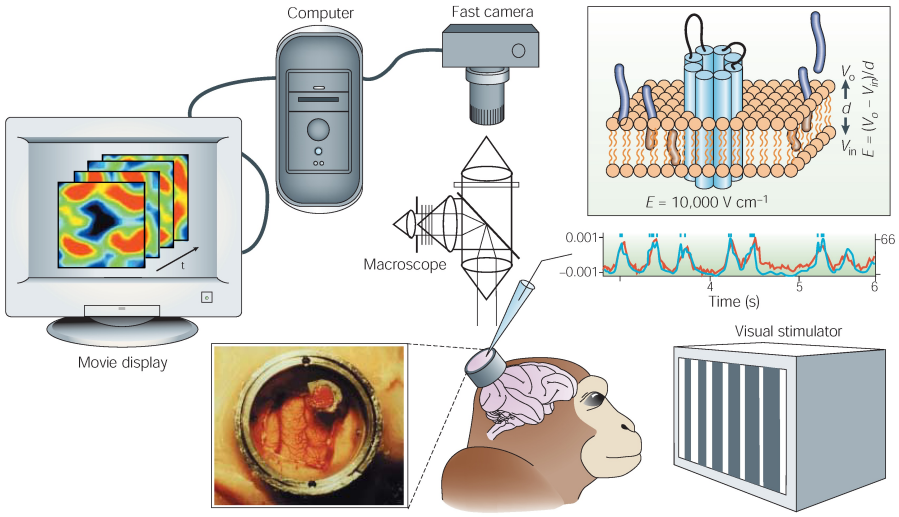

Figure 3.3: Voltage Sensitive Dye Imaging

3.2.3 Combining two techniques

VSD imaging has been employed to investigate long-range cortical connections and the propagation of cortical activity in vivo, and it has been used to measure large-scale changes in cortical activity following brain injury such as stroke or following sensory deprivation in the barrel cortex. While structural connectivity

can identify long-range connections, such as the connection between the barrel cortex and motor cortex, VSD imaging can be used to further investigate the spatiotemporal dynamics of the connection [11].

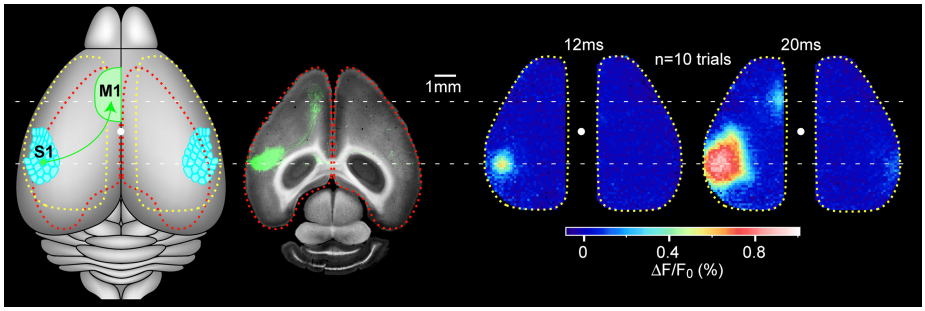

Figure 3.4: Functional connectivity detection using VSD. A stimulation at the associated S1 region turns a remote area (M1) on. Taken from [11] with courtesy

For this essay we have used the data coming from Timothy Murphy Lab[1]. They have used transgenic mice that predominantly express ChR2 in layer 5 pyramidal neurons. Mice were given a large craniotomy and the VSD response was recorded across the entire hemisphere (Lim et al., 2012). Using galvanometer mirrors to steer a 473 nm laser to various cortical regions, we were able to activate any area of the cortex, including less-studied regions like the parietal association cortex or secondary cortices[11].

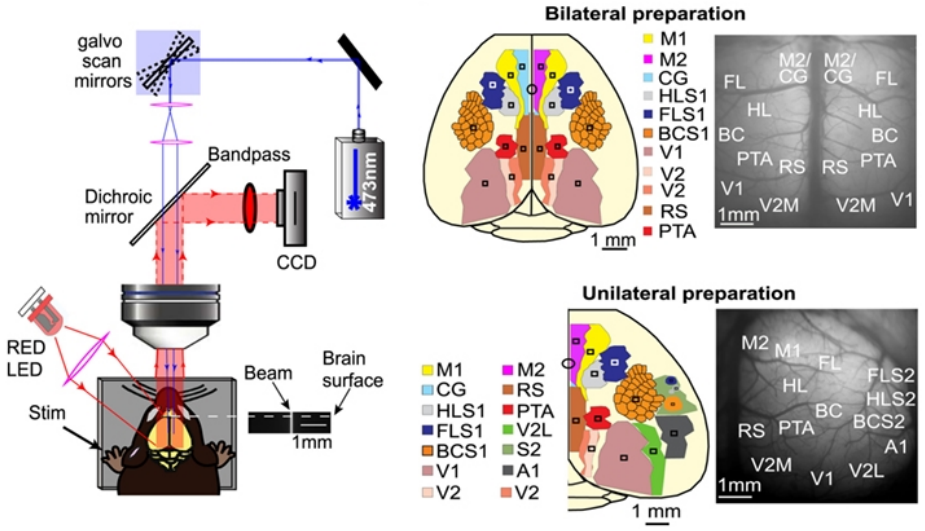

Figure 3.5: Functional connectivity detection using VSD. A stimulation at the associated S1 region turns a remote area (M1) on. Taken from [11] with courtesy

The VSD response was recorded for both hemispheres and the strength of the response at specific regions of interest was calculated to estimate the strength

[1]University of British Columbia

of the connections between various regions of interest. From this, we were able to calculated the strength of connections between regions and create a network diagram to quantitatively display the strength of connections between regions. A very interesting power that fast functional imaging gave us was the ability to study time-dependent functional connectivity. Figure 3.6 demonstrates such a study where we could determine the functional connectivity network at different times after stimulations.

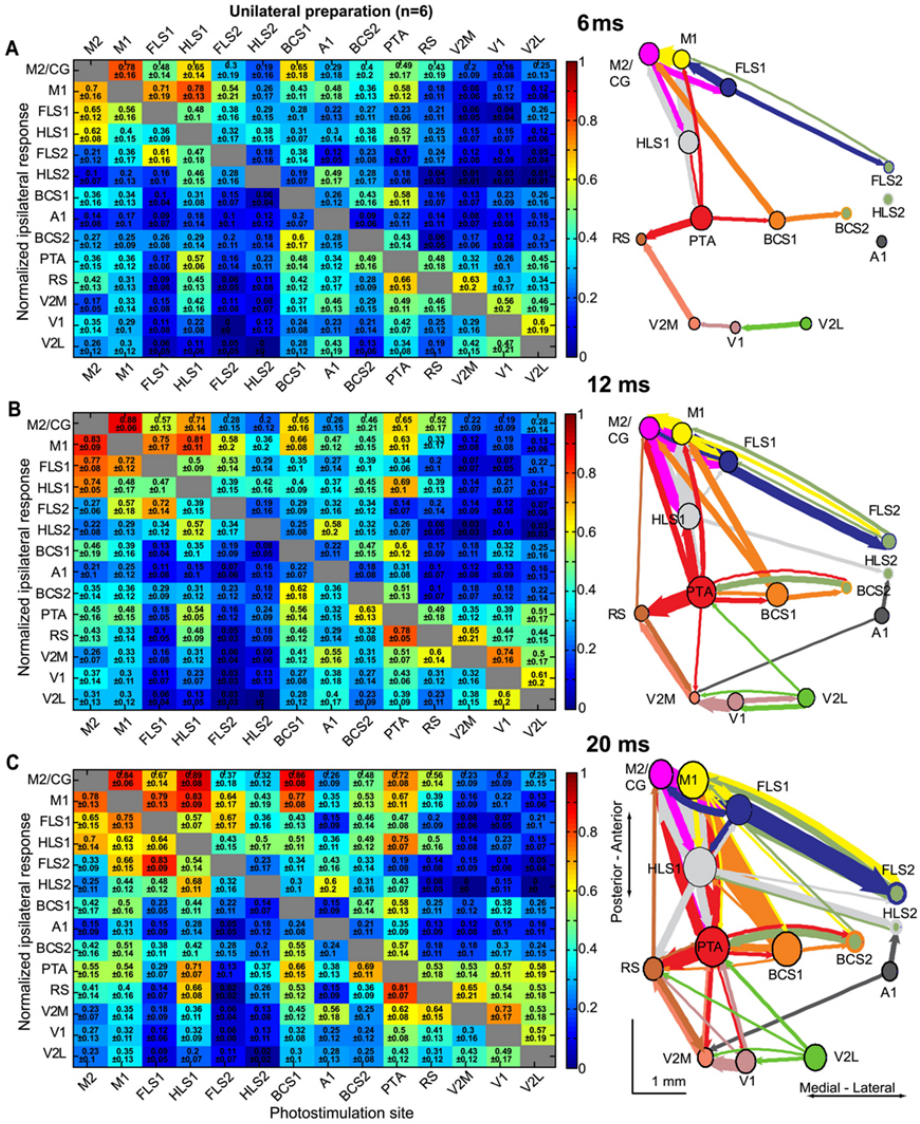

Figure 3.6: Time-Dependent Functional Connectivity: connectivity changes over millisecond timescales after direct cortical photostimulation.[11]

Network analysis revealed a number of interesting points: We identified regions that are highly connected to many other regions (*hub regions*), regions with few connections, and asymmetrical connection strength between regions

(See Figure 3.7.a). For example, the connections from primary to secondary sensory areas were significantly stronger than the reciprocal connections (from secondary to primary sensory areas), suggesting more driver connections in the bottom-up direction than in top-down. The role of thalamic feedback loops or subcortical contribution to the VSD signal remain unclear when using this method.

The combination of VSD imaging and ChR2 stimulation has the advantage of high spatial and temporal resolution for stimulating and recording, and can be done quickly and relatively non-invasively compared to traditional cortical probing methods that rely on electrical stimulation.

3.3 Communicability Analysis of VSD + Optogenetics Data

Let us begin our analysis by looking at the pre- and post-stroke connectivity matrices that we have measured using VSD + Optogenetics technique. Figure 3.7.a shows the connectivity matrix of a healthy mouse where the upper left corner of the matrix shows ipsilateral connectivity in left hemisphere ($L \rightarrow L$). The bottom right corner represents ipsilateral connectivity in right hemisphere ($R \rightarrow R$). The other two corners show the contralateral connectivity between two hemispheres ($L \rightarrow R$ and $R \rightarrow L$).

Figure 3.7.b shows the connectivity matrix 8 weeks after a focal stroke induced at right fore-limb cortex (FLR) denoted with red boxes. We observe that the connectivity map has changed dramatically where we have a significant reduction in $R \rightarrow R$ and a remarkable increase in $L \rightarrow L$ connectivity.

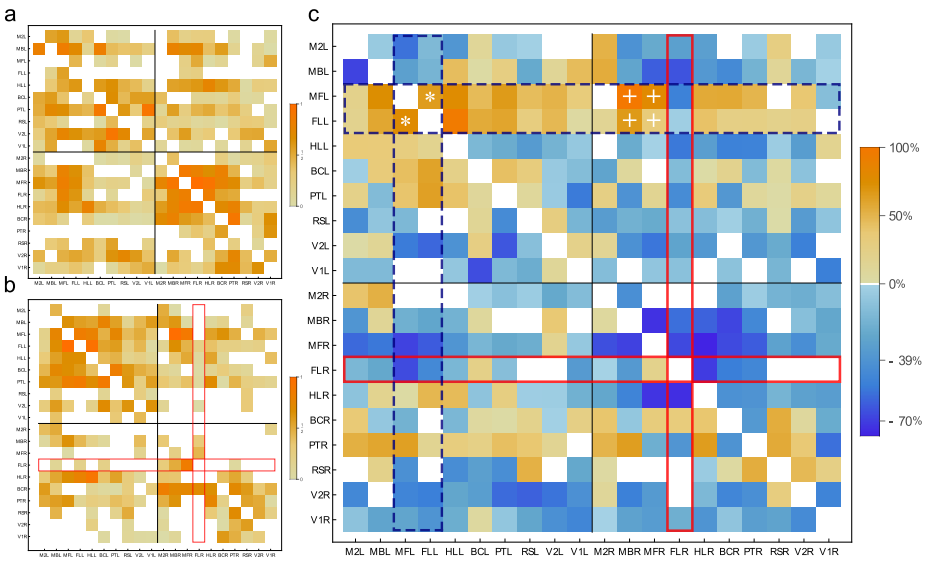

Figure 3.7: (**a**)Connectivity matrix of healthy mouse cortex (**b**) Connectivity matrix after stroke in Right Fore-Limb (FLR) shown by red boxes (**c**)change in connectivity after 8-weeks. Red box shows the damaged area and the dashed box shows the contralateral are- Left Fore-Limb (FLL)

Figure 3.7.c shows the percentage of change in connectivity before and after stroke where blue squares represent links with reduced connectivity (that are dominant) and orange ones show the opposite where connectivity has increased.

One may point many interesting physiological observations from this experiment. Here we stress a few:

- There has been a marked increase in the functional connectivity at the opposite hemisphere and not much of a recovery in the damaged one.
- the highest percentage of increase is at the exact sensory and motor counterpart of the infarct (shown by the dashed boxes).

One possible interpretation could be that, the brain is trying to recover the altered function of right fore-limb using the similar connectivity pattern at its left hemisphere counterpart. One interesting observation is the remarkable cross-connectivity of left sensory and motor areas (denoted by *). On the other hand, brand new connections have also appeared between between sensory and motor contralateral areas (shown by +). It seams that the brain tries to recover sensory-motor function of the damaged hemisphere by connecting it to the intact one.

A crucial decision to be made is how we are going to interpret the measured connectivity matrix. Does it simply represent the weighted adjacency graph of the network as many studies have assumed ? Our previous results on Estrada communicability and TEC tell us that the activity correlation between nodes of a network is not simply identical to the adjacency matrix. In our experimental case, the entries of connectivity matrix say a_{ij} show the relative signal amplitude received at node v_j from v_i and does not imply a direct anatomical connection. Thus we interpret the connectivity matrix as some form of communicability matrix instead of taking it as the adjacency matrix of the network.

Recovering the network using communicability distance matrix binarization as we introduced in Section 2.2 gives interesting results as shown in Figure 3.8.

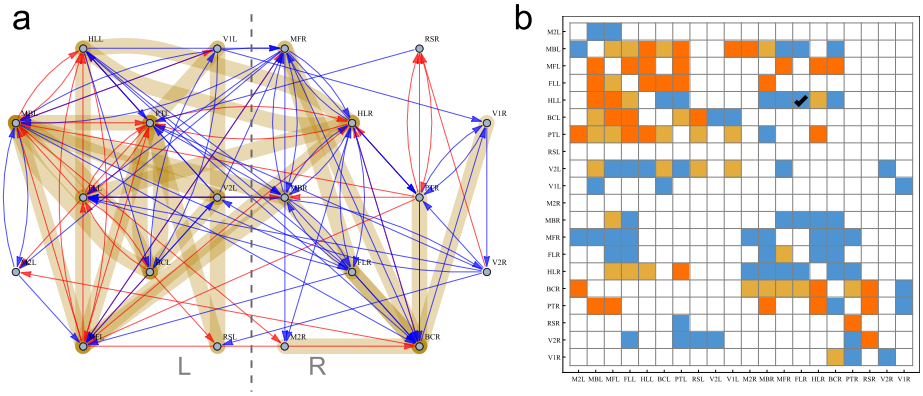

Figure 3.8: (**a**)obtained graph of anatomic connectivity. Blue: The lost links, Red: New links, Brown: Unchanged. There are some brown+(red/blue) edges overlapping. Actually some of these connections were 2-way and now only one remains. (**b**) Adjacency matrix after stroke- changes in connectivity after 8-weeks. Blue: Lost links, Red: New links, Brown: Unchanged

We observe that although based on the work of Crofts et al. [9] , physical connectivity in both hemispheres decrease after stroke, the functional connectivity in the opposite cortex increases significantly. These results suggest that the brain compensates the damage in long-range connections (white matter) with increased cortical connectivity.

Acknowledgments

It is a pleasure to thank my mentor, Professor Porter who without his advice this work was not possible.

Bibliography

[1] Porter, Mason . A Terse Introduction to Networks. Springer, 2013.

[2] Newman, Mark, Albert-Laszlo Barabasi, and Duncan J. Watts. The structure and dynamics of networks. Princeton University Press, 2011.

[3] Estrada, Ernesto, and Naomichi Hatano. "Communicability in complex networks." Physical Review E 77.3 (2008): 036111.

[4] Estrada, Ernesto, Naomichi Hatano, and Michele Benzi. "The physics of communicability in complex networks." Physics Reports 514.3 (2012): 89-119.

[5] Higham, Nicholas J. Functions of matrices: theory and computation. Siam, 2008.

[6] Crofts, Jonathan J., and Desmond J. Higham. "A weighted communicability measure applied to complex brain networks." Journal of The Royal Society Interface 6.33 (2009): 411-414.

[7] Estrada, Ernesto. "The communicability distance in graphs." Linear Algebra and its Applications 436.11 (2012): 4317-4328.

[8] Seung, Sabastion. "I Am My Connectome." Video file retrieved from: http://www. ted. com/talks/sebastian seung. html (2010).

[9] Crofts, J. J., et al. "Network analysis detects changes in the contralesional hemisphere following stroke." Neuroimage 54.1 (2011): 161-169.

[10] Grinvald, Amiram, and Rina Hildesheim. "VSDI: a new era in functional imaging of cortical dynamics." Nature Reviews Neuroscience 5.11 (2004): 874-885.

[11] Lim, Diana H., et al. "In vivo large-scale cortical mapping using channelrhodopsin-2 stimulation in transgenic mice reveals asymmetric and reciprocal relationships between cortical areas." Frontiers in neural circuits 6 (2012).

[12] Deisseroth, Karl. "Optogenetics." Nature methods 8.1 (2010): 26-29.